The regularities of the formation of carbon nanostructures from hydrocarbons based on the composition of the reaction mixture

Ilya V. Mishakov [a,b,c], Yuri I. Bauman [a], Ivan A. Streltsov [a], Denis V. Korneev [d],
Olga B. Vinokurova [e], Aleksey A. Vedyagin [a,c,*]

[a] *Boreskov Institute of Catalysis SB RAS, Novosibirsk, Russian Federation*
[b] *Novosibirsk State University, Novosibirsk, Russian Federation*
[c] *National Research Tomsk Polytechnic University, Tomsk, Russian Federation*
[d] *State Research Centre of Virology and Biotechnology VECTOR, Novosibirsk, Russian Federation*
[e] *Institute of Solid State Chemistry and Mechanochemistry SB RAS, Novosibirsk, Russian Federation*

Abstract

This paper presents the results of research on the regularities of the formation of carbon nanofibrous materials, as well as the influence of the composition of the model mixture of hydrocarbons C_1–C_4 on the morphological features and textural characteristics of the resulting carbon nanofibres (CNF).

One of the most urgent issues faced by the oil and gas industry is how to increase the processing depth of associated petroleum gas (APG). In the Russian Federation alone, the annual economic losses from unutilised APG during processing are estimated at 2 billion dollars. It is known that the composition of APG can vary greatly, depending on the oil and gas field. In particular, the methane concentration, the main component of natural gas and associated gas, varies from 25 to 95 vol.%. In this study, we sought to identify the main factors that determine the morphology and structure of CNF, and to develop approaches in processing actual hydrocarbon mixtures to produce a carbon product with the desired or predictable characteristics. Such an approach can serve as a basis for resource-saving catalytic technology utilizing C_1–C_4 hydrocarbons that are currently disposed of as post-combustion flare gas.

The research results clearly demonstrate that the morphology and texture of the carbon materials obtained by the decomposition of hydrocarbon mixtures depend on the composition of the reaction gas. The key components in this case are methane and the resultant hydrogen: their relationship at a specific temperature determines the direction of the reversible reaction of carbon hydrogenation: $C + 2H_2 = CH_4$.

The decisive factor in the decomposition of hydrocarbons yielding carbon materials is the degree of deviation of the methanation reaction from equilibrium which can be influenced in two ways. The addition of hydrogen to the reaction gas promotes the driving force of the carbon hydrogenation reaction, resulting in defective high-surface carbon fibres. Increasing the concentration of methane in the reaction gas composition, in contrast, reduces the driving force of methanation until the process is suppressed, which promotes a more structured form of the CNF, without defects.

1. Introduction

The synthesis of carbon nanofibres (CNF) and nanotubes (CNTs) on nickel-containing catalysts from raw hydrocarbons is of paramount practical importance [1–4]. This method, known by the acronym CCVD (Catalytic Chemical Vapour Deposition), along with valuable carbon nanomaterials, produces pure hydrogen, and has generated recent interest as a potential method for effectively processing natural gas based on methane and associated petroleum gas (APG) [5–8]. One of the most urgent issues faced by the oil and gas industry is how to increase the processing depth of associated petroleum gas (APG). In the Russian Federation alone, the annual economic losses from unutilised APG during processing are estimated at 2 billion dollars.

* Corresponding author. Boreskov Institute of Catalysis SB RAS, Novosibirsk, Russian Federation. Tel.: +7 383 326 96 60; fax: +7 383 330 74 53.

E-mail address: vedyagin@catalysis.ru (A.A. Vedyagin).

It is known that in terms of its properties, methane differs significantly from all other representatives of the homologous series of hydrocarbons. An important property of the molecule CH_4 is its high stability [9,10]. It is known that the reaction of methane decomposition into carbon (graphite) and hydrogen is endothermic, whereas all other hydrocarbons decompose exothermically. Methane decomposition up to very high temperatures (900 °C or higher) is reversible, which implies the simultaneous presence in equilibrium conditions of both methane and hydrogen [11]. The equilibrium level of methane conversion increases with temperature, but this is almost always accompanied by a thermodynamic limit, which prohibits the attainment of 100% conversion of methane with the formation of CNF and hydrogen.

It is known that the composition of the reaction medium has a decisive influence on the morphology and structure of carbon fibres formed by the decomposition of hydrocarbons [12]. We should also note another important fact: the catalytic decomposition of any hydrocarbons C_2–C_n forming carbon and hydrogen will always generate side reactions in the hydrogenation of the carbon to form methane (methanation). Our previous studies have shown [13–15] that methanation plays a key role in the "loosening" of the packing of graphene layers in the body of the fibre, causing the formation of "feathery" nanofibres with a high specific surface area.

$$C + 2H_2 \rightleftarrows CH_4 \qquad (1)$$

In the temperature range of the decomposition of hydrocarbon mixtures under study (400–800 °C), the reaction (1) is reversible. This explains the occurrence of a driving force for the hydrogenation of carbon, which to some extent is manifested with the decomposition of all hydrocarbons except methane itself.

During the decomposition of a mixture of propane and butane, the formation of hydrogen takes place according to the reaction Eqs. (2) and (3).

$$C_3H_8 \rightarrow 3C + 4H_2 \qquad (2)$$

$$C_4H_{10} \rightarrow 4C + 5H_2 \qquad (3)$$

Thus, we can delineate several fundamentally important factors that together will determine the structural features of the resulting carbon materials:

1 the methane concentration in the composition of the hydrocarbon mixture (APG);
2 the conversion rate of raw hydrocarbon; and
3 the temperature for carrying out the process.

Some influence may also be wielded by other additives in the composition of natural gas (molecular nitrogen, carbon dioxide, etc.), hydrocarbon diluent, but their total concentration in the composition of APG rarely exceeds 10 vol.%, which means that their contribution is minor.

By increasing the degree of the conversion of raw hydrocarbon, the hydrogen concentration increases, thereby "launching" the methanation reaction, which in turn is reflected in the nature of the structuring (the number of defects) of the carbon fibres, and therefore, their textural and morphological characteristics.

2. Materials and methods

For the synthesis of CNF we used a nickel–copper catalyst with the following composition: 84 wt.% NiO + 13 wt.% CuO + 3 wt.% Al_2O_3. The catalyst was prepared through the mechanochemical activation of nickel oxide (II), copper oxide (II) and aluminium hydroxide, combined in the corresponding ratio. Mechanochemical activation was carried out in an AGO-3 planetary mill (grinding medium – steel balls with a diameter of 8 mm, the acceleration of the grinding medium – 390 m/sec², activation time – 15 mins).

Before beginning the experiment on the synthesis of CNF the catalyst was reduced in the hydrogen stream at 550 °C for 15 minutes. The reduction led to the formation of dispersed particles of Ni–Cu alloy, which subsequently played a role of the active centres for the carbon fibre growth [15–17]. Aluminium oxide in an amount of 3 wt.% serves the function of a structural promoter, preventing the sintering of alloyed metal particles [15].

To investigate the dependence of the morphology and texture properties of the carbon material on the composition and degree of conversion of raw hydrocarbon, experiments were conducted in a horizontal flow-through quartz reactor. The specially-designed reactor allowed us to carry out a so-called "discrete load" of the catalyst – in several different consecutive points (up to five) along the length of the reactor.

The experimental reactor was a horizontal 1.4 m tube made of quartz, with two main entry–exits at the ends, as well as 9 add-ons, used for sampling the gas phase along the length of the reactor while the hydrocarbons were in the decomposition process.

A schematic of the reactor with the reaction insert for the discrete catalyst load is presented in Fig. 1. The catalyst was discretely loaded into the reactor by 4 equivalent samples.

The catalyst was placed at the liner surface in separate samples (5 mg each, with 15–20 cm increments) so that the sample was situated in the reactor zones at approximately the
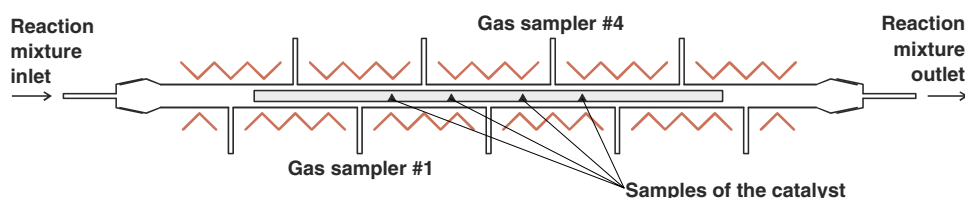

Fig. 1. Scheme of a horizontal quartz reactor with a discrete catalyst loading.

same temperature (±2 °C). The reactor was heated in an argon stream to a predetermined temperature, the catalyst reduction was performed by supplying hydrogen, and then introducing the reaction mixture containing hydrocarbons. The hydrocarbon raw material used in the experiment was household gas C_2–C_4 (3.5 vol.% C_2H_6, 81.5 vol.% C_3H_8, 6.6 vol.% n-C_4H_{10} and 8.4 vol.% i-C_4H_{10}) and/or natural gas (92 vol.% CH_4).

The composition of reaction gas at the exit from the intermediate samplers (No. 1, No. 4) was analysed using a "CHROMOS" dual-channel gas chromatograph with a flame ionisation detector. The synthesis of the carbon material lasted 40 minutes. At the end of the experiment, the resulting product was cooled in an argon stream, the insert was removed from the reactor, and unloading was performed for each CNF sample one by one to prevent them from mixing with each other.

We applied transmission electron microscopy (TEM) at an accelerating voltage of 80 kV using a JEM-1400 JEOL microscope (Japan) to study the morphological characteristics of the carbon product.

Low temperature nitrogen adsorption (BET method) was used to measure the textural parameters of the resulting materials (specific surface, pore volume). Our method for calculating the textural characteristics was based on an analysis of the nitrogen adsorption isotherms at 77 K. Measurements were performed on an automated device – the ASAP-2400 (Micromeritics, USA).

3. Results and discussion

Fig. 2 shows the results of the measurement of the specific surface area of carbon materials according to the location of the catalyst sample in the reactor. In the experiment, the model mixture was C_2–C_4, with no methane content. As seen in Fig. 2, the specific surface of the CNF samples increases with the distance of the catalyst sample from the entrance into the reactor. Table 1 shows the chromatographic analysis of the composition of the reaction mixture (samples No. 1 and No. 4).

An analysis of the gas phase showed that as a result of the decomposition of the initial mixture C_2–C_4, besides the hydrogen,

Table 1
Results of the analysis of the reaction mixture composition (Sample No. 1 and No. 4).

Component	Concentration, vol.%	
	Sample no. 1	Sample no. 4
Hydrogen	0	53.6
Methane	0	9.2
Ethylene	0	1.0
Ethane	3.5	3.2
Propane	81.5	27.9
Butane (iso-butane and n-butane)	15.0	5.1

the formation of methane (9.2 vol.%) and small amounts of ethylene (1 vol.%) occurs. The total conversion of hydrocarbons at the time sample No. 4 is attained reaches 36%. The increase in the hydrogen concentration along the length of the reactor (from 0 to 53.6 vol.%) results in the formation of a carbon product with a large surface area due to an increase in the contribution of the methanation process.

The following result shows that the effect of the methanation reaction can be suppressed by the addition of methane (natural gas) into the reaction mixture C_2–C_4. As shown in Fig. 3a 45 vol.% addition of natural gas to the reaction stream leads to a marked decrease in the specific surface area of the samples of carbon materials. This upward trend of S_{BET} over the length of the reactor is maintained.

The increase in the concentration of hydrogen in the reaction zone leads to an opposite effect. Thus, the addition of hydrogen to the reaction mixture of C_2–C_4 intensifies the methanation process and, as a consequence, results in a product with a greater specific surface (Fig. 4). The concentration of H_2 in the feed mixture was 42 vol.%. The specific surface area of the CNF sample reaches maximum values and changes in the range of 220–305 m^2/g.

For more obvious demonstration of the influence of the process of carbon hydrogenation on the textural characteristics
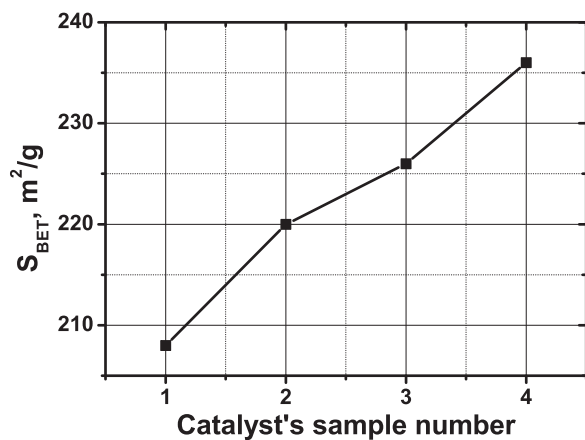

Fig. 2. Dependence of the specific surface of CNF samples on the location of the catalyst sample in the horizontal tubular reactor. Decomposition of the C_2–C_4 mixture over the Ni–Cu/Al_2O_3 catalyst at 600 °C.
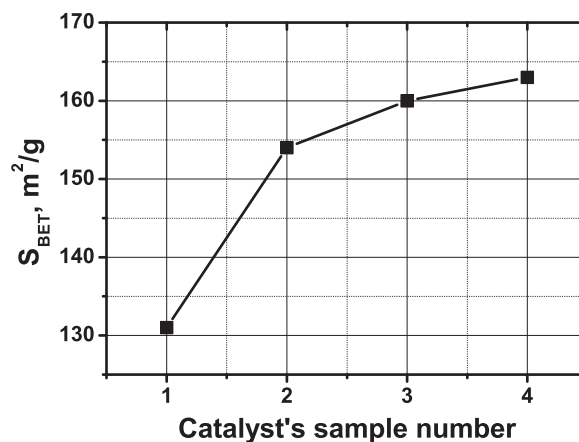

Fig. 3. Dependence of the specific surface area of the CNF samples on the location of the catalyst sample in the horizontal tubular reactor. Decomposition of the model mixture C_2–C_4 (55 vol.%) and natural gas (45 vol.%) over the Ni–Cu/Al_2O_3 catalyst at 600 °C.
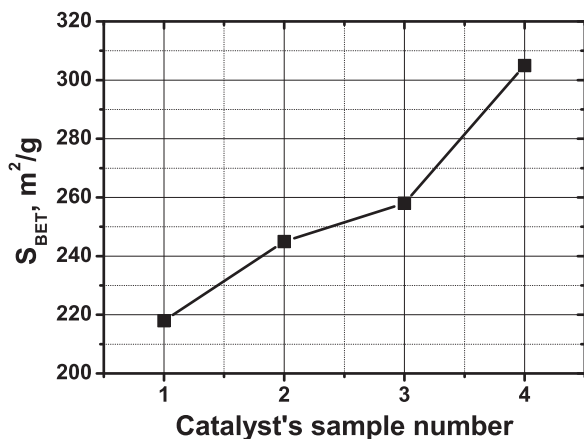
Fig. 4. Dependence of the specific surface area of CNF samples on the sample location in the horizontal tubular reactor. Decomposition of the model mixture C_2–C_4 (58 vol.%) and hydrogen (42 vol.%) over the Ni–Cu/Al_2O_3 catalyst at 600 °C.

of the resulting carbon product, we plotted the specific surface area of the samples against the value of the product work of the methanation reaction, calculated according to Eq. (4):

$$PW = \frac{p_{CH_4}}{p_{H_2}^2} \qquad (4)$$

where PW is the product work, atm^{-1};

$p(H_2)$ is partial pressure of hydrogen in the mixture, atm;
$p(CH_4)$ is partial pressure of methane in the mixture, atm.

Fig. 5 shows the dependency graph of the specific surface area values of CNF samples based on PW and data from various experiments. For all samples, the product work was calculated from the results of an analysis of the gas composition supplied to the corresponding sample of carbon material. One can see that changes in the composition of the reaction mixture to decrease the values of the PW (i.e., by increasing the driving force for the methanation reaction) lead to an increase in the
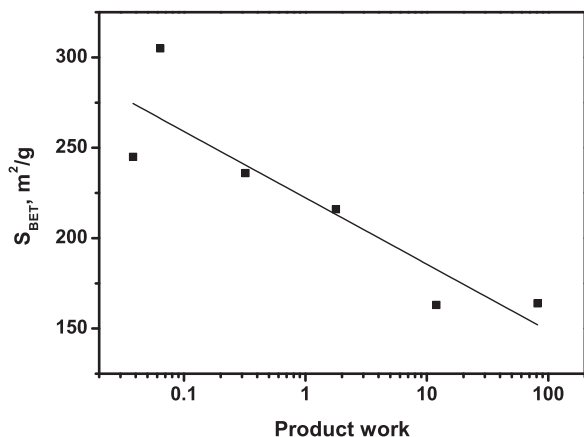

Fig. 5. Dependence of the specific surface area of the CNF samples on the product work (PW) of methanation reaction. The calculations for PW values are based on the data from the chromatographic analysis of the composition of the reaction gas.

specific surface area of the carbon nanofibre samples and facilitates the transition of their morphology to the "feathery" type (defective packing) [13,18].

The study of the morphology of the respective CNF samples using TEM showed that, along with an increase in surface area, there is a significant change in the morphological arrangement of synthesised carbon fibres. Fig. 6 shows the TEM micrographs of carbon samples prepared by varying the composition of the reaction mixture.

It follows from the pictures that an increase in the methane concentration in the composition of the hydrocarbon mixture C_1–C_4 results in the formation of virtually defect-free carbon nanofibres with close-packed graphene layers (Fig. 6a). The decomposition of the pure mixture C_2–C_4 (without the addition of methane) leads to the formation of carbon fibres with a defective surface and uneven packing (Fig. 6b). The insertion of a hydrogen-rich additive to the reaction mixture C_2–C_4 contributes to the formation of regular feathery fibre with the loosest, most defective structure (Fig. 6c).

Next, we consider in more detail the morphological features of carbon fibres produced in the catalytic decomposition of a wet fraction of natural gas (C_2–C_4 hydrocarbons). As shown above, the absence of CH_4 in the feed reaction mixture determines the course of the hydrogenation reaction of the deposited carbon, leading to the formation of fibre with a loose, feathery structure.

Fig. 7 shows an extended fragment (L ~ 12 μm) of carbon fibre formed over ~20 minutes of the reaction. The fibre's growth rate, according to our estimates, is ~0.6 μm/min. The image also shows the concentration of methane and hydrogen at the start and end of the fibre growth.

Fig. 8 shows a set of TEM images that display in detail the dynamics of change in the morphology of the carbon fibre, as shown in Fig. 7. It is evident that the initial growth stage of carbon fibre (Fig. 8a) is characterised by a sufficiently ordered packing of graphene layers (platelet type). This section of the fibre corresponds to the first minutes of its growth ($\tau = 1 \div 5$ min), when the concentration of CH_4 is close to zero, and the proportion of H_2 does not exceed 5 vol.% in the gas phase because of the low conversion of C_2–C_4 hydrocarbons.

Fig. 8b and c corresponds approximately to the middle of the length of the analysed fragment carbon fibre ($\tau = 9 \div 14$ min). It is evident that, with the nanofibre growth, we see the gradual increase in loosening of the packing of graphene layers. The edges of the fibres become more defective (with "notches"), and the level of structuredness falls. It should also be noted that its diameter decreases with growth, i.e. the fibre gets thinner. This is explained by the fact that the active particle of the Ni–Cu alloy catalysing the fibre growth gradually loses its active component due to disintegration with the formation of finer particles. One of these particles can be seen in Fig. 8c (a black spot).

The set of the last three TEM images (Fig. 8d–f) corresponds to the "tail" of the carbon fibre ($\tau = 15 \div 20$ min). Obviously, the structure of the fibre is increasingly defective: it is composed of piles of individual packings of graphene with multiple spaces in the pack. The thread grows thinner by almost 2 times,
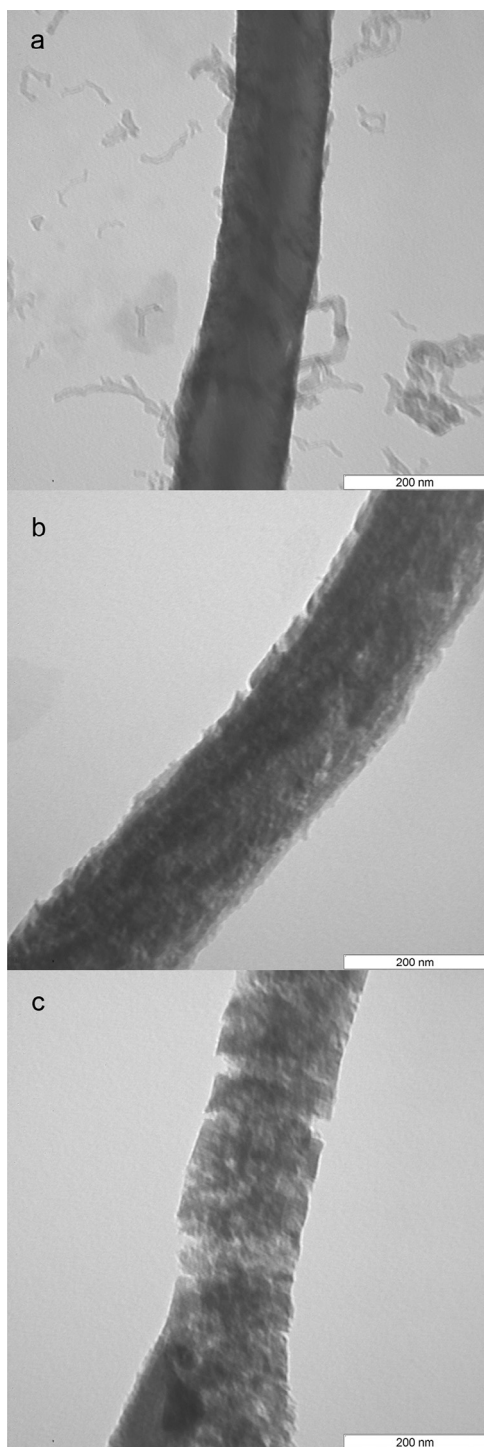
Fig. 6. TEM pictures of carbon fibres obtained over the Ni–Cu/Al$_2$O$_3$ catalyst at 600 °C by decomposition of:
a – model mixture C$_2$–C$_4$ (55 vol.%) and natural gas (45 vol.%), S$_{BET}$ = 131 m^2/g;
b – model mixture C$_2$–C$_4$, S$_{BET}$ = 211 m^2/g;
c – model mixture C$_2$–C$_4$ (58 vol.%) and hydrogen (42 vol.%), S$_{BET}$ = 305 m^2/g.

dividing into separate "threads", finer fibres. Presumably, this occurs as a result of the crushing of the initial metallic particle Ni–Cu alloy into smaller fragments, which further act as independent active centres of CNF growth.
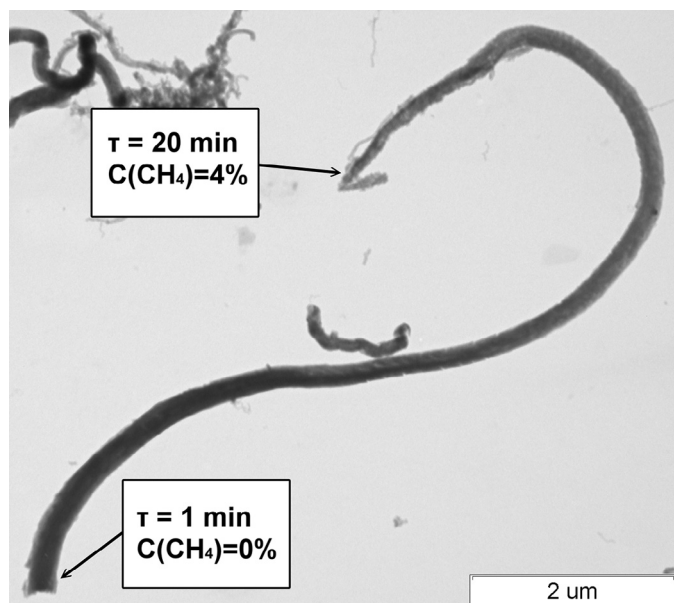

Fig. 7. TEM image of carbon fibre obtained during the changing composition of the reaction medium. Decomposition of the model mixture C$_2$–C$_4$ over the Ni–Cu/Al$_2$O$_3$ catalyst at 600 °C.

In the final phase of the growth of the carbon fibre, when its morphology almost completely corresponds to the feathery type, using chromatographic analysis, the increase in methane concentration was fixed at 9 vol.%, and hydrogen at 54 vol.%. This result proves that the growing contribution to the reaction of carbon methanation is crucial for the formation of loose, defective carbon fibres with high textural characteristics. The effect of the methanation reaction on the morphology of carbon fibres is expressed in the formation of a large number of defects in the structure, which occur as the result of the "wasting away" of individual graphite fragments due to carbon hydrogenation. The structural disorder of feathery fibres, which determines the high textural characteristics of the carbon material, is a result of the intermittent nature of the diffusion of carbon atoms through the metal particle.

The character of the structuring (loosening, defects) of the resulting carbon product is determined by the degree of deviation of the carbon hydrogenation reaction from equilibrium. Numerically, the driving force of the reaction (Δ) is expressed as the difference between the value of the equilibrium constant of the reaction at a given temperature (C$_E$) and the current value of the product work (PW):

$$\Delta = C_E - PW \tag{5}$$

The PW is calculated using the Eq. (4).

Let us consider three different situations.

1 $\Delta > 0$. The steady tendency towards the formation of defective carbon fibres with high specific surface area (CNF of feathery type).

This means that under these conditions there is a tendency in the reaction behaviour to form methane, i.e. the depletion of hydrogen on carbon hydrogenation. In the case where the initial concentration of C(CH$_4$) = 0, $\Delta = C_E$, since PW = 0, and therefore,
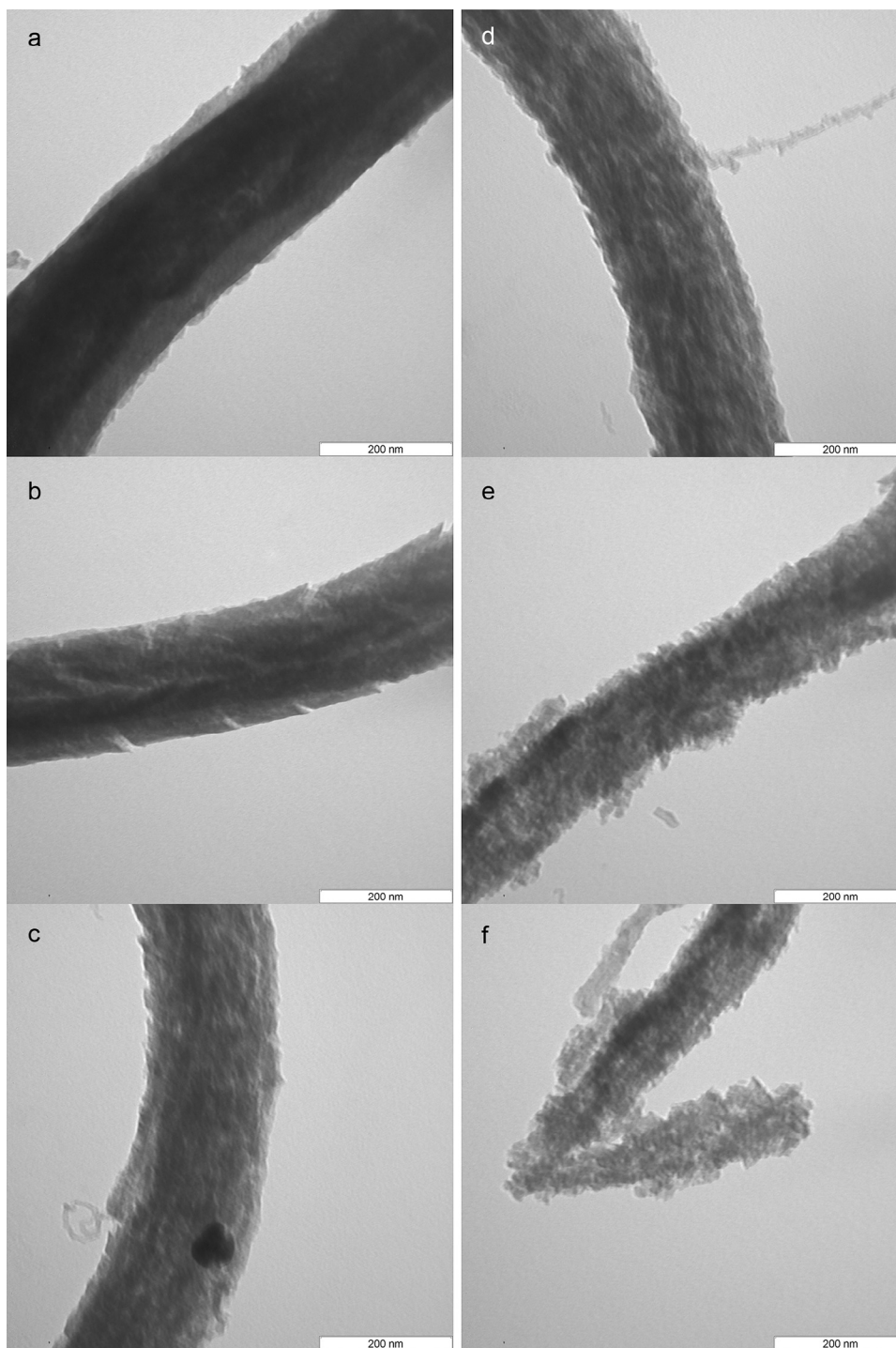
Fig. 8. TEM images of the various sections of carbon fibre shown in Fig. 7.

the driving force of the methanation reaction is maximal. For example, at 600 °C, the driving force will be 2.02 atm^{-1}, which coincides with the theoretical value of the equilibrium constant.

2 $\Delta < 0$. The area of the formation of highly ordered carbon nanofibres.

Under these conditions, the reverse reaction of methane decomposition into carbon and hydrogen will predominate. The reaction of carbon hydrogenation will be suppressed. Such a case results from the decomposition of natural and associated gas with a high methane content (70–95 vol.%). The further the system is from the equilibrium reaction $CH_4 = C + 2H_2$, the smaller the contribution of the carbon hydrogenation reaction and so, consequently, the more perfect the nature of the packing of graphene layers in the resulting body of carbon fibres.

3 $\Delta \sim 0$. Carbon fibres are formed with an intermediate structure.

When $\Delta \sim 0$, the system $CH_4 = C + 2H_2$ is close to equilibrium, when neither one nor the other reaction is clearly dominant. The decomposition of methane and its formation by methanation may be seen as conditionally equally probable processes. In such conditions, the formation of carbon nanofibres with an intermediate structure occurs, the morphology of which cannot be clearly attributed to a particular type of CNF.

4. Conclusions

This article summarises the results of experimental studies aimed at establishing the regularities of the formation of carbon materials in various conditions of the catalytic conversion of hydrocarbon mixtures. Hydrocarbons of natural origin (natural gas, associated gas) are often a mixture with a rather complex composition. Typically, they are always present in varying concentrations of methane and hydrocarbons C_2–C_4. Therefore, we had to establish a relationship of the basic characteristics of carbon materials (and morphological texture) with the composition of hydrocarbons from which they are derived.

A specially organised experiment in a horizontal flow-through reactor with discrete catalyst loading allowed us to establish the main tendencies in the changes of the texture and morphology of carbon materials, depending on the composition of the model mixture of hydrocarbons C_1–C_4. The following sets out the basic conclusions resulting from our research.

The process of the decomposition of a mixture of hydrocarbons C_1–C_4 can lead to the formation of three fundamentally different variants of CNF:

- *Structured* carbon fibres (Type 1);
- *Defective* carbon fibres with a pinnate morphology (Type 2);
- Carbon fibres *with an intermediate structure* (Type 3).

The first type of carbon fibres is formed by the decomposition of mixtures with a high content of methane (70–90 vol.%). The morphology of the fibres is characterised by a high degree of ordering and the right character of the packing of graphene layers.

The second type of carbon fibres can be obtained by the breakdown of the fraction of hydrocarbons C_2–C_4, by a small concentration of methane in the reaction stream, and also with the addition of hydrogen to the reaction gas.

The third type of carbon material in terms of morphological properties occupies an intermediate position between the first and second types of CNF.

The main cause of defective carbon fibres with a feathery morphology is the reaction of carbon hydrogenation to form methane (methanation). We found that the degree of disorder is correlated with the driving force of the methanation reaction (Δ) defined as the degree of deviation of this reaction from equilibrium conditions. The value of the parameter Δ depends on the temperature and the ratio of methane and hydrogen concentrations in the reaction zone. The addition of methane to the reaction stream reduces the value of the driving force of methanation until its complete suppression, while the influence of hydrogen has the exact opposite effect.

References

[1] S.-P. Chai, S.H.S. Zein, A.R. Mohamed, Synthesizing carbon nanotubes and carbon nanofibers over supported-nickel oxide catalysts via catalytic decomposition of methane, Diam. Relat. Mater. 16 (2007) 1656–1664.

[2] K. Otsuka, Y. Abe, N. Kanai, Y. Kobayashi, S. Takenaka, E. Tanabe, Synthesis of carbon nanotubes on Ni/carbon-fiber catalysts under mild conditions, Carbon 42 (2004) 727–736.

[3] Y. Shen, A.C. Lua, Sol-gel synthesis of titanium oxide supported nickel catalysts for hydrogen and carbon production by methane decomposition, J. Power Sources 280 (2015) 467–475.

[4] M.A. Ermakova, D.Y. Ermakov, Ni/SiO$_2$ and Fe/SiO$_2$ catalysts for production of hydrogen and filamentous carbon via methane decomposition, Catal. Today 77 (2002) 225–235.

[5] A.E. Awadallah, A.A. Aboul-Enein, A.K. Aboul-Gheit, Various nickel doping in commercial Ni-Mo/Al$_2$O$_3$ as catalysts for natural gas decomposition to CO$_x$-free hydrogen production, Renew. Energy 57 (2013) 671–678.

[6] J.L. Pinilla, M.J. Lázaro, I. Suelves, R. Moliner, Formation of hydrogen and filamentous carbon over a Ni–Cu–Al$_2$O$_3$ catalyst through ethane decomposition, Appl. Catal. A Gen. 394 (2011) 220–227.

[7] Y. Wang, N. Shah, G.P. Huffman, Simultaneous production of hydrogen and carbon nanostructures by decomposition of propane and cyclohexane over alumina supported binary catalysts, Catal. Today 99 (2005) 359–364.

[8] H. Wang, R.T.K. Baker, Decomposition of methane over a Ni-Cu-MgO catalyst to produce hydrogen and carbon nanofibers, J. Phys. Chem. B 108 (2004) 20273–20277.

[9] W.M. Sackett, The thermal stability of methane from 600 to 1000 °C, Org. Geochem. 23 (1995) 403–406.

[10] J. Majewska, B. Michalkiewicz, Carbon nanomaterials produced by the catalytic decomposition of methane over Ni/ZSM-5: significance of Ni content and temperature, New Carbon Mater. 29 (2014) 102–108.

[11] U.P.M. Ashik, W.M.A. Wan Daud, H.F. Abbas, Production of greenhouse gas free hydrogen by thermocatalytic decomposition of methane – a review, Renew. Sust. Energ. Rev. 44 (2015) 221–256.

[12] S. McCaldin, M. Bououdina, D.M. Grant, G.S. Walker, The effect of processing conditions on carbon nanostructures formed on an iron-based catalyst, Carbon 44 (2006) 2273–2280.

[13] I.V. Mishakov, R.A. Buyanov, V.I. Zaikovskii, I.A. Strel'tsov, A.A. Vedyagin, Catalytic synthesis of nanosized feathery carbon structures via the carbide cycle mechanism, Kinet. Catal. 49 (2008) 868–872.

[14] I.V. Mishakov, I.V. Strel'tsov, Y.I. Bauman, A.A. Vedyagin, R.A. Buyanov, High surface carbon nanofibers: features of synthesis and morphology, Univ. Bull. Chem. Chem. Technol. 54 (2011) 107–110 (in Russian).

[15] I.A. Strel'tsov, O.B. Vinokurova, I.V. Tokareva, I.V. Mishakov, V.P. Isupov, Y.V. Shubin, et al., Effect of the nature of a textural promoter on the catalytic properties of a nickel–copper catalyst for hydrocarbon processing in the production of carbon nanofibers, Catal. Ind. 6 (2014) 176–181.

[16] M.C. Diaz, J.M. Blackman, C.E. Snape, Maximising carbon nanofiber and hydrogen production in the catalytic decomposition of ethylene over an unsupported Ni-Cu alloy, Appl. Catal. A Gen. 339 (2008) 196–208.

[17] O.Y. Podyacheva, Z.R. Ismagilov, A.E. Shalagina, V.A. Ushakov, A.N. Shmakov, S.V. Tsybulya, et al., Structural changes in a nickel–copper catalyst during growth of nitrogen-containing carbon nanofibers by ethylene/ammonia decomposition, Carbon 48 (2010) 2792–2801.

[18] I.V. Mishakov, V.V. Chesnokov, R.A. Buyanov, A.L. Chuvilin, Morphology and structure of carbon formed from chlorohydrocarbons on nickel–cobalt containing catalysts, React. Kinet. Catal. Lett. 76 (2002) 361–367.